SiGe/Si superlattice power generators

Gehong Zeng, John E. Bowers
Department of Electrical and Computer Engineering, University of California, Santa Barbara, CA 93106
Yan Zhang, and Ali Shakouri*
Electrical Engineering Department, University of California-Santa Cruz , 1156 High Street, Santa Cruz, CA 95064
*Corresponding Email: ali@soe.ucsc.edu, phone: (831) 459-3821

Abstract

SiGe is one of the best thermoelectric materials for high temperature applications. Superlattice structures can further enhance the thermoelectric properties by reducing the thermal conductivity and by increasing the Seebeck coefficient via selective emission of hot electrons through thermionic emission. SiGe/Si superlattice structures were grown on a silicon wafer using molecular beam epitaxy. A single element SiGe/Si superlattice thermoelectric power generator was fabricated and characterized. The device element, a 3 μm thick SiGe/Si superlattice on a 3.95 μm SiGe buffer layer, was grown on 5 inch diameter 650 microns thick silicon substrate. Output power of 0.1 W/cm^2 with a resistive load was measured with a temperature drop of 220°C across the generator element. There was a significant parasitic lead resistance. Simulations show that if the temperature drop is increased to 300°C, a power density of 1 W/cm^2 can be achieved when working in impedance matching condition.

Introduction

The performance of thermoelectric devices is largely dependent on the material figure-of-merit $Z = \alpha^2\sigma/\kappa$, where α is the material Seebeck coefficient, σ electrical conductivity and κ thermal conductivity. For thermoelectric applications, Bi_2Te_3, Sb_2Te_3 or Bi_2Se_3 are commonly used when working around room temperatures, and their dimensionless figure-of-merit ZT has a value around unity when the material is optimized. For high temperature applications, SiGe has been used, and its ZT values can be close to unity at high temperatures. Aside from its good thermoelectric properties, it is compatible with standard silicon circuit growth and fabrication processes, which makes it very competitive compared to other thermoelectric materials[1,2]. A large figure-of-merit Z is necessary for high power densities and high efficiency levels. It is believed that low dimensional structures could overcome the efficiency barriers imposed by the physical limit of conventional bulk materials[3-5]. In 1993, Hicks and Dresselhaus first proposed using low dimensional semiconductor structures to enhance thermoelectric properties[6,7]. Our SiGe/Si superlattice micro-refrigerator experimentally demonstrated an enhanced cooling of 4.5 °C, about four times that of bulk silicon devices[8]. The superlattice interfaces provide phonon scattering centers to reduce cross-plane thermal conductivity[9]. Furthermore, electron filtering by periodic superlattice barriers can also enhance the cross-plane Seebeck coefficient, where only hot electrons with high enough energy could go through. Non-planar barriers and embedded quantum dot structures are suggested to achieve high thermoelectric conversion efficiency[10]. The figure-of-merit $Z = \alpha^2\sigma/\kappa$ for superlattice structures can be improved through carrier pocket engineering by increasing the power factor $\alpha^2\sigma$ and reducing thermal conductivity κ[11,12]. Thus, improvements on material thermoelectric properties could enhance the power output and energy conversion efficiency for thermoelectric generators.

Power generation from a variety of heat sources has been studied intensively[13-17]. Here we report the fabrication and characterization of SiGe/Si superlattice power generators.

Material structures and characterization

A 3 μm SiGe/Si epitaxial layer along with 3.95 μm SiGe graded buffer layer were grown on a 650 μm silicon substrate using (MBE). As SiGe has a larger lattice constant than silicon, a buffer technique was employed to solve the problem by using graded SiGe in place of unstrained SiGe or strain-compensated SiGe/Si superlattice materials[1,18]. The thermal conductivity of the SiGe/Si superlattice is ~10 $Wm^{-1}K^{-1}$ measured by 3ω technique by Majumdar's group in UC Berkeley[9].

The cross-plane Seebeck coefficient of SiGe/Si superlattice was measured in our lab. In order to measure the cross-plane Seebeck coefficient of a SiGe/Si superlattice, a thin film heater was fabricated on top of the superlattice mesa to apply a heat source. The temperature difference ΔT and its Seebeck voltage output V can be measured directly. The Seebeck coefficient could be calculated by the equation, $\alpha = V/\Delta T$. The Seebeck coefficient of 420 μV/K for the SiGe/Si superlattic was measured. We described the detailed methodology and technique elsewhere[19, 20].

Device structure and fabrication

The generator was designed to work with an 800K heat source and a room temperature heat sink. The temperature difference built across the device element generates thermoelectric power when connected to an external electric load. The schematic of the power generator system is shown in Fig. 1.

The generator element consists of a 3 μm SiGe/Si superlattice along with a 3.95 μm graded SiGe buffer layers on a 650 μm silicon substrate. 650 μm thick AlN were used for the upper and the lower plates. The temperature will drop across upper, lower AlN plates and device element as well as the interfaces between upper AlN plate and heat source, and lower AlN plate and heat sink. To characterize the device performance, the temperature difference across the device element ($\Delta T_{Element}$) is of special interest due to the fact that the Seebeck coefficient of the element material can be expressed as $\alpha = \Delta V/\Delta T_{Element}$, where the ΔV is the output voltage. Two

metal wire thermal sensors were integrated in the generator for an in situ temperature measurement. The device structure is shown in Fig. 2.

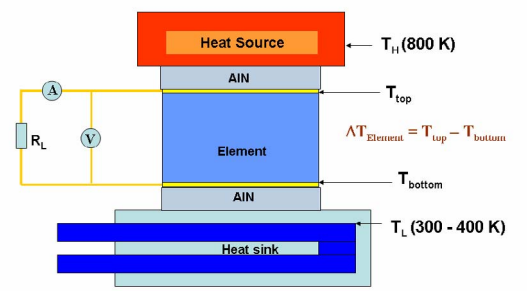

Figure 1: Schematic diagram of power generator system.

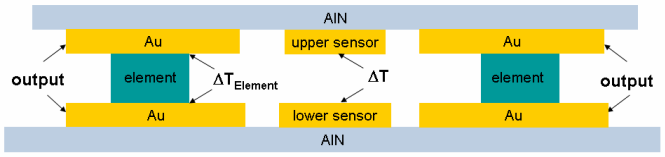

Figure 2: Schematic structure diagram of power generator with built-in thermal sensor for in situ temperature measurements

A Cr/Au layer was used for the metal wire sensors which were patterned on the upper and lower AlN plates respectively. A thick Au layer was also deposited on the plates as bonding pads for Au-Au diffusion bonding with the SiGe/Si elements. Ti/Al layers were deposited on both sides of the SiGe/Si element as contact metallization and annealed at 450 °C for 5 seconds. Using the transfer length method (TLM), we measured the contact resistances between Au-contact layer and the element, ranging from 6.5×10^{-7} to 3×10^{-7} Ωcm^2 when the temperature varyed from 25 to 250 °C. After annealing, additional Ti/Au layers were deposited on top of the previous Ti/Al metal layers on both sides of the element, and used for Au-Au fusion bonding pads with the AlN plates.

Measurement Results and Analysis

The measurement setup consists of a temperature controlled heat sink and four multimeters which are computer-controlled via GPIB. Two of the multimeters were used for the temperature measurement of the upper and lower plates via the two in situ thermal sensors; the other two were used for the output voltage and current measurements respectively. The generator was placed on a heat sink, and a copper bar was placed on its top. The heat source was from the flame of a butane torch. The measurement set-up is illustrated in Fig.3.

The upper and lower sensors were calibrated before device measurement. The calibrations were done in an electric oven with temperature management facilities. To reduce the variations of calibration, the upper and lower sensors were calibrated using four wire resistance measurements at the same time. The calibration modular is shown in Fig.4

The temperature sensitivity of the sensor can be expressed as $\frac{dR}{dT} = \frac{l}{w \cdot d} \cdot \frac{d\rho}{dT}$, which depends on the properties of the sensor material as well as the metal wire geometry, where l is the length, w the width, d the thickness and ρ the resistivity. Given a $\frac{d\rho}{dT}$, the temperature sensitivity can be increased by increasing the sensor wire length, using thin film or narrow sensor wire. Because the linearity of temperature versus resistance for Au is excellent from room temperature to 600 °C[19], the calibrations were carried out from 20 to 80 °C. Due to their different geometry, the sensitivities are about 0.2524 Ω/K and 0.20404 Ω/K for upper and lower sensors respectively.

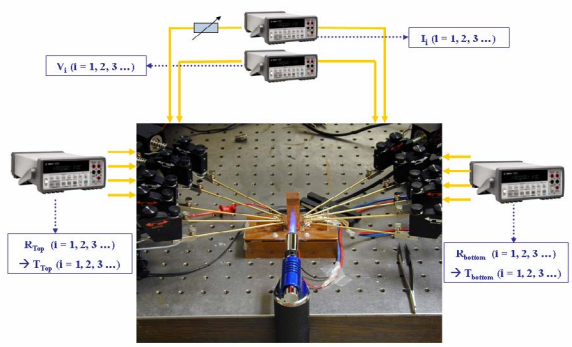

Figure 3: The measurement setup to measure the output power.

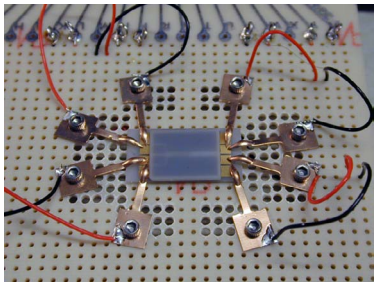

Figure 4: The temperature versus resistance calibration of the upper and lower sensors were carried out at the same time using four wire resistance measurement.

As shown in Fig.2, the actual temperature dropping across the device element $\Delta T_{Element}$ is smaller than ΔT, the temperature difference between the upper and lower sensor.

By comparing the results of output voltage versus temperature from different measurement methods, the $\Delta T_{Element}$ can be determined. During generator measurement, the temperature difference between the two thermal sensors ΔT and the voltage output ΔV can be obtained. An effective Seebeck coefficient can be expressed as $\alpha_{effective} = \Delta V / \Delta T$; while the actual Seebeck coefficient of the element material is as $\alpha = \Delta V / \Delta T_{Element}$. As the actual element Seebeck coefficient α of the element is known via Seebeck test pattern device measurement, and the Seebeck coefficient of Au or AlN is negligible, the actual temperature dropping between the

element ($\Delta T_{Element}$) can be known. In our experiments, the ratio of $\Delta_{TElement}$ / ΔT for measured devices is about 1/3.

The output power of 16 mW/cm^2 was measured for generators of 1 mm^2 elements when the temperature difference between the upper and lower plate reaches about 160 °C. The measurement results are shown in Fig. 5.

The output power is proportional to $R_L \cdot (\frac{\alpha \cdot \Delta T}{r + R_L})^2$, where α is the Seebeck coefficient of the element, ΔT is the temperature difference across the two thermal sensors, r is internal resistance and R_L is the electric load. If the temperature difference dropping is increased, the output power will be enhanced significantly. The quadratic fitting on the measured results is shown in solid curve in Fig.5. The extrapolation indicates that the output power can reach up to 50 mW/cm^2 when the temperature difference ΔT increases to 300 °C.

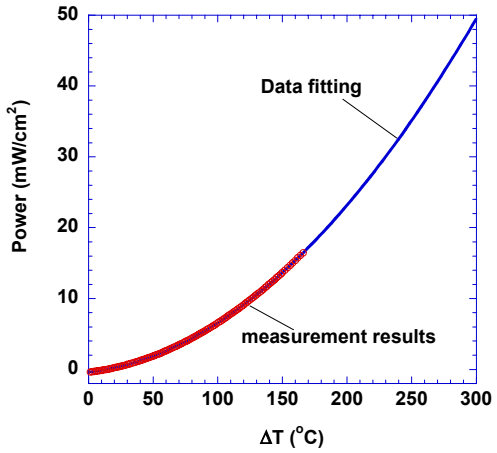

Figure 5: The dots are represented the measurement results from 1 mm^2 device. Quadratic fitting on the measurement results with temperature difference increased to 300 °C.

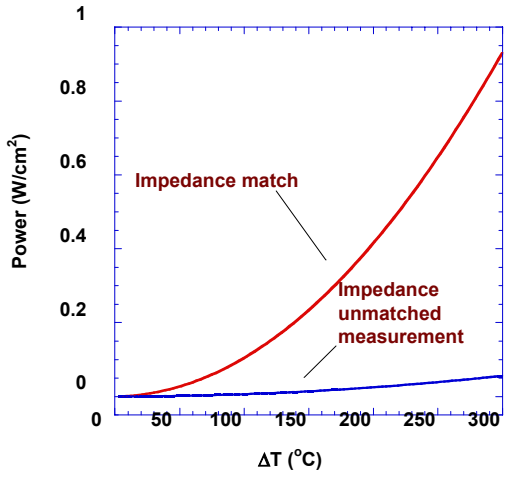

Figure 6: The comparison of output power at resistance match conditions (R_L = r) and measurement results in impedance unmatched conditions (r = 0.09Ω, R_L = 5.8Ω).

The internal resistance r of the device is about 0.09Ω, which includes contact resistance, element material resistance, metal layer resistance and parasitic resistance from Au to Au fusion bonding interfaces. Our external effective electric load R_L is about 5.8Ω, which consists of the resistance from the conduct lead, the probe, and the input circuitry of a multimeter in current measurement mode. The output power generated in the current set-up is measured under mismatched load condition, where $R_L >> r$. As we know, the maximum output power could only be achieved at an impedance match condition, where $R_L = r$. If we implement matched load condition in our set-up, we could expect a much higher output power. Fig.6 compares the output power of the matched load condition ($R_L = r$ = 0.09Ω) with the mismatched condition (R_L=5.8Ω, r=0.09Ω) versus the temperature gradient ranging from 0 to 300°C.

Conclusions

SiGe/Si superlattice generators were fabricated and tested. In situ temperature sensors were integrated in the device to measure the working temperatures. The generators were measured in a test setup, including four multimeters, a temperature controlled heat sink. Cross-plane Seebeck coefficients about 420 μV/K were measured for the SiGe/Si superlattice structure. Output electrical power up to 16 mW/cm^2 was measured for packaged generators of 0.6 mm × 1 mm^2 elements in impedance unmatched conditions. High power density of 1 W/cm^2 is predicted when the generator works in impedance match conditions with a temperature gradient of 300°C. A future measurement using a load capable of matching to the milliohm resistance of the element is underway.

Acknowledgments

This work is supported by the Office of Naval Research Thermionic Energy Conversion Center MURI monitored by Dr. Mihal E. Gross. The authors would also like to acknowledge Kian-Giap Gan, and Manish Mehta for their help in the programming for measurement and device element dicing respectively.

References

[1] X. Fan, G. Zeng, C. LaBounty, J. E. Bowers, E. Croke, C. C. Ahn, S. Huxtable, A. Majumdar, and A. Shakouri, Applied Physics Letters **78,** 1580-1582 (2001).

[2] X. Fan, Ph.D. Thesis, University of California, 2002.

[3] M. J. Kelly, Low-dimensional semiconductors : materials, physics, technology, devices (Oxford University Press, New York, 1995).

[4] V. A. Markel and T. F. George, Optics of Nanostructured Materials (Wiley Series in Lasers and Applications) (Wiley-Interscience, 2000).

[5] T. M. Tritt, Recent Trends in Thermoelectric Materials Research Iii **71,** Ix-Xiv (2001).

[6] L. D. Hicks, T. C. Harman, and M. S. Dresselhaus, Applied Physics Letters **63,** 3230-3232 (1993).

[7] L. D. Hicks and M. S. Dresselhaus, Physical Review B **47,** 12727-12731 (1993).

[8] X. Fan, G. Zeng, E. Croke, C. LaBounty, C. C. Ahn, D. Vashaee, A. Shakouri, and J. E. Bowers, Electronics Letters **37,** 126-127 (2001).

[9] S. T. Huxtable, A. R. Abramson, C. L. Tien, A. Majumdar, C. LaBounty, X. Fan, G. H. Zeng, J. E. Bowers, A. Shakouri, and E. T. Croke, Applied Physics Letters **80,** 1737-1739 (2002).

[10] Vashaee and A. Shakouri, Physical Review Letters **92,** - (2004).

[11] T. Koga, X. Sun, S. B. Cronin, and M. S. Dresselhaus, Applied Physics Letters **75,** 2438-2440 (1999).

[12] T. Koga, X. Sun, S. B. Cronin, and M. S. Dresselhaus, Applied Physics Letters **73,** 2950-2952 (1998).

[13] D. M. Rowe, Renewable Energy **5,** 1470-1478 (1994).

[14] D. M. Rowe, Applied Energy **40,** 241-271 (1991).

[15] L. G. Chen, J. Z. Gong, F. R. Sun, and C. Wu, International Journal of Thermal Sciences **41,** 95-99 (2002).

[16] Z. H. Dughaish, Physica B-Condensed Matter **322,** 205-223 (2002).

[17] I. H. Kim, Materials Letters **43,** 221-224 (2000).

[18] G. Zeng, A. Shakouri, C. La Bounty, G. Robinson, E. Croke, P. Abraham, X. Fan, H. Reese, and J. E. Bowers, Electronics Letters **35,** 2146-2147 (1999).

[19] Gehong Zeng, John E. Bowers, Yan Zhang, Ali Shakouri, Joshua Zide, Arthur Gossard, Woochul Kim and Arun Majumdar, "ErAs/InGaAs" superlattice Seebeck Coefficient", to be published, Proc. of ICT (2005).

[20] A. Matula, J. Phys. Chem. Ref. Data **8,** 1147 (1979).